

Article

The Effects of Feedstock, Pyrolysis Temperature, and Residence Time on the Properties and Uses of Biochar from Broom and Gorse Wastes

Eliana Cárdenas-Aguilar ^{1,2} , Ana Méndez ^{3,*} , Gabriel Gascó ¹, Marcos Lado ² and Antonio Paz-González ² 

¹ Department of Agricultural Production, Universidad Politécnica de Madrid, Ciudad Universitaria, 28040 Madrid, Spain; eliana.cardenas@upm.es (E.C.-A.); gabriel.gasco@upm.es (G.G.)

² Centro Interdisciplinar de Química e Biología CICA, University of Coruña, As Carballleiras, s/n Campus de Elviña, 15008 Coruña, Spain; marcos.lado@udc.es (M.L.); antonio.paz.gonzalez@udc.es (A.P.-G.)

³ Department of Geological and Mining Engineering, Universidad Politécnica de Madrid, 28040 Madrid, Spain

* Correspondence: anamaria.mendez@upm.es

Featured Application: Biochars from broom and gorse presented appropriate properties for use as fuels for energy production and pose no risks from an environmental perspective due to their low PAH content. These biochars are rich in carbon and have a low ash content. However, future investigations are needed to optimize and better understand their use in energy production and other potential uses, for example, as reductant materials in carbothermic reduction processes.

Abstract: Biochar (BC), which can be produced from several feedstocks, has been widely studied. However, the BC derived from highly pyrolytic shrubs, such as broom and gorse, has been less frequently used and only partially characterized. These wastes, when used for the preparation of biochar, can fix carbon and contribute to environmental conservation, helping to achieve sustainable development objectives. Eight biochars from broom and gorse were produced and fully analyzed, providing a more complete and novel description, with new insights for assessing their utilization. The aims of this study were to elucidate the effects of feedstock, pyrolysis temperature, and residence time on biochar properties and to assess the adequacy of these biochars as fuel. Elemental and proximate analyses and estimations of the lower and higher heating values were performed, and physical and chemical properties, as well as several other related energy indices, were determined. The experimental results showed that the temperature was a key factor in the properties of the biochars, while residence time was less important. The BCs obtained from the two feedstocks did not show important effects on the properties, which is consistent with the fact that they are woody legumes. These biochars had a high carbon content and were thermally stable. The BCs also had a high calorific value and suitable energetic properties. Additionally, their PAH contents were low, indicating that the use of these biochars would be safe. In conclusion, broom- and gorse-derived biochars can be considered as renewable fuels for green energy production.

Keywords: biochars; broom; gorse; waste; valorization



Citation: Cárdenas-Aguilar, E.; Méndez, A.; Gascó, G.; Lado, M.; Paz-González, A. The Effects of Feedstock, Pyrolysis Temperature, and Residence Time on the Properties and Uses of Biochar from Broom and Gorse Wastes. *Appl. Sci.* **2024**, *14*, 4283. <https://doi.org/10.3390/app14104283>

Academic Editor: Anna Stoppato

Received: 26 March 2024

Revised: 3 May 2024

Accepted: 15 May 2024

Published: 18 May 2024



Copyright: © 2024 by the authors. Licensee MDPI, Basel, Switzerland. This article is an open access article distributed under the terms and conditions of the Creative Commons Attribution (CC BY) license (<https://creativecommons.org/licenses/by/4.0/>).

1. Introduction

Biochar (BC) is a carbonaceous material that results from the pyrolysis of biomass in an inert atmosphere or in the limited presence of air [1]. The dominant factors that influence the physicochemical properties of biochar and its end applications are the feedstock type and the thermochemical parameters, namely, pyrolysis temperature, residence time, and heating rate [2,3].

BC can be produced from a variety of organic feedstocks, including sewage sludge [4], animal manure [5–7], deinking paper sludge [8], and pruning waste [9], among others. Different feedstocks result in differences in the physical and chemical properties of biochar.

Lignocellulosic biomass, which includes agricultural residues, forest debris, and industrial waste, is receiving interest due to its profuse availability and low cost. Commonly, lignocellulose waste is categorized into two main classes: woody and herbaceous or nonwoody waste [10–12]. Woody plants have a relatively higher lignin content, but herbaceous plants have higher cellulose and hemicellulose contents. Therefore, the biomass from herbaceous plants has lower thermal stability, and their macromolecules undergo carbonization more easily during pyrolysis. These wastes, when used for the preparation of biochar, can fix carbon and contribute to environmental conservation, helping to achieve sustainable development objectives.

Regarding pyrolysis conditions, in general, BC production is conducted via slow pyrolysis, which typically takes place using a heating rate of $<2\text{ }^{\circ}\text{C s}^{-1}$; slow pyrolysis can produce comparatively high-quality BC with a stable carbon content and a low H/C ratio. Temperature has a significant effect on the physicochemical properties of BC, including its functional groups, surface area, and porosity. Previous investigations showed that the temperature of slow pyrolysis mostly varies between 300 and 600 $^{\circ}\text{C}$ depending on the intended BC use [3,5,13]. Residence times may vary from minutes to days; a moderate-length residence time is required to optimize the biochar production both in terms of yield and physicochemical properties [11,14]. Common gorse (*Ulex europaeus*, L.) and scotch broom (*Cytisus scoparius*, L. (Link)) are evergreen nitrogen-fixing shrubs belonging to the legume family; gorse is a spiny or thorny plant. Both shrubs are distributed worldwide, either as native or introduced species. As a native species, gorse is most abundant along the western coast of Europe and in the British Isles [15], and it is widespread near the western Mediterranean Sea. Scotch broom, as a native species, is most common in central Europe and the British Isles, from Ireland to Ukraine, and from southern Spain to southern Norway [16,17]. Both legume shrubs have been widely introduced around the world for different reasons. According to the International Union for Conservation of Nature, introduced stands of gorse and broom are most abundant in maritime regions at temperate latitudes, in the United States, Canada, South Africa, New Zealand, and Australia [18–23]. They are also established at subtropical latitudes, for example, in several mountains areas from India and Brazil [24,25], and on islands such as Hawaii [26] and Reunion [27]. As an invasive species, gorse and Scotch broom have been recorded in 52 and 54 countries and islands, respectively [22,23].

Although several beneficial attributes of gorse and broom have been identified, they are now viewed as prolific seeders that escaped from cultivation and had become invasive species and noxious weeds in most of the countries to which they have been introduced. Moreover, even though these species have been present in European countries for centuries, they are often considered a weed due to their several detrimental effects [28].

On the other hand, the positive effects of these shrubs are associated with their ability to fix nitrogen. Additionally, they have some secondary beneficial effects like their use as hedges or ornamental plants [19,27] and natural herbicides [29], and for their medicinal or immunological value [30]. Gorse was historically used as fuel in the British Isles; in northwest Spain and northern Portugal, it has been extensively mixed with animal waste to make fertilizer. In addition, gorse has been used as fodder and broom for cleaning purposes in several regions worldwide. Nowadays, these traditional uses, however, have been abandoned, leading to increased biomass availability [15,30].

The harmful effects of gorse and Scotch broom are associated with their ability to form dense impenetrable monospecific stands that affect the dynamics of the landscape; modify the edaphic composition; reduce or even eliminate native grasslands, forests, rangelands, and agricultural lands areas; and create fire hazards [21,31]. Moreover, serious fire hazards can affect both the invasive and native ranges of gorse and Scotch broom, because these shrubs are highly flammable and produce high residual biomass [31–33]. For example, the shrub communities in the European region of Galicia, Spain, and northern Portugal, belonging both to the Euro-Atlantic and Mediterranean biogeographic domains, are abundant. In this region, gorse and broom are prone to severe wildfires, which have intensified in

recent decades [34–36]. The surface areas of gorse and broom in this European region have been estimated at about 530,000 and 470,000 ha, respectively [37]. Fuel loads have been measured in Galicia, yielding aerial biomass values of 33.6 ± 14.5 and 53.7 ± 36.0 t ha⁻¹ for gorse and broom, respectively. Additionally, the total measured fuel load amounts, including litter, are 40.0 ± 22.8 for gorse and 61.9 ± 47.3 t ha⁻¹ for broom. In addition, frequently gorse, but also broom, occurs under Pinus and Eucalyptus forests, which are also subjected to fire hazards. The risk of wildfires could be drastically reduced if this available and abundant low-cost aerial biomass is used as feedstock to synthesize renewable sources of energy, including biochar.

Characterizations of BC from woody feedstocks including trees [38], tree by-products such as wood chips [39], wood industry residues such as sawdust [40], or pruning waste [3,9] are widely available. Similarly, several invasive herbaceous species have been broadly used as biochar feedstock in several applications [41]. Selected examples are (i) *Ambrosia artemisiifolia* L., used as a metal-accumulating biochar in order to treat potentially toxic elements (PTEs) [42]; (ii) *Eupatorium adenophorum* biochar, which reduced the Pb and Cd contents from aqueous solutions, leading to possible use in heavy metal remediation [43]; and (iii) *Ambrosia trifida* L., converted to biochar and used as an effective adsorbent for the treatment of Trichloroethylene (TCE)-contaminated groundwater, which is the predominantly occurring chlorinated hydrocarbon in groundwater in industrial/urban areas around the world [44]. For fuel production, the ideal invasive species is *Spartina alterniflora* due to its high productivity and heat value [45].

However, despite the wide distribution of gorse and broom across much of the temperate and subtropical agroecological landscapes of the world, research on the valorization of its biomass produced via modern thermochemical conversion techniques has been rather limited. The valorization of gorse as a potential renewable energy source (fuel or electricity) has been addressed [46,47], and the use of broom [48] and gorse [49] for fuel production has been also explored. Notably, a characterization of torrefaction products from both gorse and broom was reported [50].

Overall, the characterization of gorse- and Scotch broom-derived BC has received comparatively less attention than that of BC from forest species or invasive herbaceous plants. As a result, the former two biochars have been only partially described, and their full characterization still is lacking. Even if the biochar obtained from gorse [51] and broom [52] has been used for ameliorating agricultural and forest soil properties, respectively the scarce existing BC characterization research has mainly focused on the effect of pyrolysis conditions on selected BC properties. For example, Kaal et al. [53] reported elemental analyses, pyrolysis chromatograms, and FTIR diagrams for gorse BC. Similarly, Gómez et al. [51] used gorse biochar for chromium removal.

Therefore, the literature shows that the characterization of gorse- and broom-derived biochar and the suitability of these shrubs to produce fuel have been insufficiently analyzed. To bridge this gap, biochars from broom and gorse were produced at two different temperatures and residence times. Elemental analysis, proximate analysis, and analysis of several chemical and physical properties were carried out in triplicate; particular attention was paid to the estimations of higher heating value (HHV) and other energy indices of the elemental composition, because they can be viewed as indicators of the amount of heat released by a fuel, as we are dealing with pyrolytic species [54,55]. In addition, PAHs were quantified. The aim of this study was to elucidate the effects of feedstock, pyrolysis temperature, and residence time on the different properties of broom- and gorse-derived biochar. In addition, the adequacy of the use of these biochars as fuels was assessed. Compared to previous studies, the novelty of our work lies in that we provide a more complete characterization of the general properties of broom and gorse BCs, as well as new insights into the valorization of these materials for their use as fuels.

2. Materials and Methods

2.1. Feedstock Selection

The feedstocks selected for this work were broom and gorse. Both species are typical vegetation in Galicia and were obtained from the Coruña region, in the northwest of Spain. Both plants are legumes of the Fabaceae family. The species were selected due to (i) their wide distribution, covering a vast area of shrubland and forest in Galicia [55]; (ii) their high pyrolytic values [54,55]. Feedstock samples were collected in May 2022. Immediately after sampling raw broom and gorse, plants were delivered to the laboratory. Humidity for broom and gorse was 54.65 ± 1.01 and $53.18 \pm 1.20\%$, respectively. Next, samples were spread out on plastic trays and air-dried for 24 h. Then, the feedstocks were dried at $60\text{ }^\circ\text{C}$ in a DIGILAN, (Labolan, Navarra, Spain) furnace for 48 h. After that, dry samples were crushed and sieved through a 4 mm sieve.

2.2. Biochar Production

The production of biochars was achieved through the slow pyrolysis of the broom and gorse samples at a $3\text{ }^\circ\text{C min}^{-1}$ heating rate in a 12-PR/400 series 8B furnace (Hobersal, Barcelona, Spain). Two pyrolysis temperatures ($300\text{ }^\circ\text{C}$ and $600\text{ }^\circ\text{C}$) and two residence times (1 h and 3 h) were set up for each material. The selected experimental conditions were chosen according to previous works [3]. Biochars derived from broom feedstock were named with BB initials followed by temperature and pyrolysis duration as follows: BB300-1H, BB300-3H, BB600-1H, and BB600-3H; biochars fabricated from gorse were similarly labeled with BG initials as BG300-1H, BG300-3H, BG600-1H, and BG600-3H.

2.3. Characterization of the Feedstock and Biochars

Biochars were milled and sieved to a particle size of less than 2 mm. For the elemental analysis, proximate analysis, and chemical property analysis, biochar samples were milled and sieved to a particle size below $200\text{ }\mu\text{m}$. Each property was measured in triplicate, except for the physical properties and PAH content, which were recorded from one representative sample.

2.3.1. Elemental Analysis

The elemental analysis (C, H, N, S) was performed by dry combustion with an elemental analyzer (FlashEA1112) (Thermo-Finnigan, San Jose, CA, USA). The oxygen (O) content was calculated as follows [56]:

$$\text{O (\%)} = 100 - (\%C + \%H + \%N + \%S + \%Ash) \quad (1)$$

The atomic ratios (H/C, O/C and ((O + N)/C)) were calculated considering the atomic weight of each element.

2.3.2. Energy Properties

The higher heating value (HHV) was estimated using four different approaches. Then, the mean value of these approaches was employed. The equations used are summarized in Table 1.

In addition, the different fuel characteristics were evaluated according to Mbugua Nyambura et al. [60] and Kongto et al. [61] for the following energy indices:

$$\text{Carbon densification factor (CDF)} = C_{\text{biochar}}/C_{\text{Feedstock}}, \quad (7)$$

$$\text{Energy enrichment factor (EEF)} = \text{HHV}_{\text{biochar}}/\text{HHV}_{\text{Feedstock}}, \quad (8)$$

$$\text{Calorific value improvement (CVI)} = (\text{EEF} - 1) \times 100, \quad (9)$$

$$\text{Energy density (ED)} (\text{MJ m}^{-3}) = \text{HHV} (\text{MJ kg}^{-1}) \times \text{Bulk density} (\text{kg m}^{-3}), \quad (10)$$

Table 1. Different estimated higher heating values (HHVs).

HHV (MJ kg ⁻¹)	Formula	Reference
HHV ₁	HHV = 0.3491*%C + 1.1783*%H + 0.1005*%S – 0.1034*%O – 0.015*%N – 0.021*%Ash (2)	[57]
HHV ₂	HHV = 32.9C + 162.7H – 16.2O – 954.4S + 1.408 (3)	[58]
HHV ₃	HHV = (0.3383*%C) + (1.422*%H) – (%O/8) (4)	[59]
HHV ₄	HHV = 0.3383*%C + 1.443(%H – (%O/8)) + (0.0942*%S) (5)	Dulong's approximation in [57]
HHV average	HHV = ((HHV ₁ + HHV ₂ + HHV ₃ + HHV ₄)/4) (6)	Present work

* All values indicate composition in % by mass on dry, ash-free basis except in the case of Equation (2), where the composition was used as a proportion.

2.3.3. Proximate Analysis

Proximate analysis was carried out using (i) a DBS-30 halogen moisture analyzer (Kern & Sohn GmbH, Balingen, Germany) for moisture content, (ii) a CR-48 furnace (Hobersal, Barcelona, Spain) for the volatile matter (VM) content, and (iii) an AAF 11/18 furnace (Carbolite Gero, Hope Valley, UK) for the ash content; finally, the fixed carbon (FC) was estimated using the following equation [62]:

$$FC (\%) = 100 - (\%VM + \%Ash), \quad (11)$$

The temperatures and times used for each process were well described in [3]. The fuel ratio (FC/VM) as well as the thermal stability (FC/(VM + FC)) were calculated [63].

2.3.4. Chemical Properties

Biochars were chemically characterized using pH, electrical conductivity (EC), easily oxidized organic carbon (C_{oxi}), and water-extractable organic carbon (WEOC). pH and EC were measured with a micro pH 2000 and micro cm 2201 conductometers (Crison, Barcelona, Spain), respectively using a solid:water ratio of 0.1:25 that was then placed in a mechanical stirrer for 1 h. C_{oxi} was determined with dichromate oxidation following the method proposed by Nelson and Sommers [64]. The WEOC was measured in the filtered solution, which was obtained by stirring 5 g of sample and 200 mL of distilled water for 1 h. The WEOC was measured in the solution with a Formacs HT analyzer (Skalar, Richmond, BC, USA).

2.3.5. Physical Properties

The pore size distribution of the biochars was measured using samples milled and sieved to a size of less than 2 mm. The equipment employed for porosity determination was a Porosimeter Auto Pore IV Mercury (Micromeritics, Norcross, GA, USA). From the measured porosity with the abovementioned equipment, the volumes of the mesopores (V_{meso}) and macropores (V_{macro}) were evaluated, and the pore diameter was assessed as mesopores if between 2 and 50 nm and macropores if >50 nm [65]. The bulk density corresponded to the weight of the biomass per volume, where the volume included the void spaces occupied by the materials [66].

The bulk densities of biochar samples and feedstock were evaluated using a metallic cylinder with a volume of 100 mL. The cylinder was filled with the dry sample and weighed. The solid density was measured with an Accupyc 1340 helium pycnometer (Micromeritics, Norcross, GA, USA). The total porosity was calculated with the bulk density and solid density by

$$\text{total porosity (\%)} = (1 - (\text{bulk density}/\text{solid density})) \times 100, \quad (12)$$

2.3.6. Polycyclic Aromatic Hydrocarbon (PAH) Content

The first step in measuring the PAH content of biochars was extraction with a microwave-assisted procedure; the process was enhanced with both constant heat and the addition of

solvent in order to improve the efficacy of the extraction. The extractant was a solution of 1:1 acetone/hexanol. Then, the clean-up of the biochars was performed [67]. The detailed process of sample quantitative determination is explained in [3]. Sixteen PAHs listed as priority pollutants by the United States Environmental Protection Agency were measured and categorized as light, medium, and heavy according to the number of aromatic rings [68].

2.3.7. Statistical Analysis

Pearson product-moment correlation analysis was used to analyze the relationship between elemental composition parameters (N, C, H, O, H/C, O/C, (O + N)/C), mean HHV, and proximate analysis parameters (VM, FC and ash content). Next, these variables were subjected to principal component analysis. Statistical analyses were carried out using the Statgraphics 19[®] Centurion version 6.03 software package.

In order to recognize the differences between samples, Duncan's test ($p < 0.05$) was performed with the results of the analysis of variance (ANOVA). For the multiple range tests, the values from the three replicates were included. The average of the samples is presented in the tables and figures along with the corresponding standard deviation. In addition, an interaction matrix was prepared for the biochars, crosschecking the properties and the pyrolysis parameters (temperature, residence time, and feedstock) with a multifactor ANOVA model.

3. Results and Discussion

3.1. Elemental Analysis

Table 2 shows the elemental analysis of the feedstock (broom and gorse) and the corresponding biochars. Among the biochars derived from broom, the N content did not statistically differ from that of the feedstock. However, for gorse biochars, the N content increased with temperature and residence time, except for BG600-3H. The nitrogen content of the broom-derived biochars was between $2.62 \pm 0.2\%$ and $3.12 \pm 0.2\%$ and was higher than that reported in previous studies [69,70]. In all cases, the C content increased with pyrolysis temperature, with BG600-3H being the sample with the highest value (72.32%). The C content of the broom-derived biochars was lower to that obtained in previous studies [69,70] and was due to the low heating rates used in our treatments. However, these biochars could be suitable for soil amelioration and C fixation [71,72]. In general, the H content of the biochars decreased with pyrolysis temperature and residence time as a result of the polymerization and condensation reactions leading to more aromatic structures and a decreased content of aliphatic groups. Related to these transformations, the O content of the biochars decreased with pyrolysis temperature and residence time for the biochars at 300 °C. No statistical differences were found in the O content of the biochars prepared at 600 °C between the two residence times. Similar results were previously obtained by different authors [50,54]. The S contents of the biochars were below 0.05% for broom and gorse materials. The S contents of the broom-derived biochars were lower in biochars than in the broom feedstock, but, in the case of gorse-derived biochars, the S content did not present statistical differences between the biochars and the feedstock.

Table 2. Elemental analyses and (O + N)/C atomic ratio (dry basis) for broom, gorse, and the biochars. Means with the same letter are not significantly different ($p > 0.05$) using Duncan's test for broom (lower case letters) and gorse (upper case letters) independently.

	%N	%C	%H	%S	%O	(O + N)/C
BROOM	2.93 ± 0.07 a,b	42.37 ± 0.31 a	5.76 ± 0.17 e	0.11 ± 0.01 b	45.67 ± 0.92 d	0.87 ± 0.01 d
BB300-1H	2.93 ± 0.26 a,b	59.4 ± 2.24 b	5.16 ± 0.06 d	0.03 ± 0 a	28.57 ± 1.79 c	0.40 ± 0.03 c
BB300-3H	3.12 ± 0.2 b	62.68 ± 1.91 b	4.81 ± 0.14 c	0.02 ± 0 a	25.04 ± 1.39 b	0.34 ± 0.02 b
BB600-1H	2.62 ± 0.2 a	68.66 ± 1 c	1.92 ± 0.14 b	0.03 ± 0 a	20.88 ± 0.37 a	0.26 ± 0 a
BB600-3H	2.63 ± 0.16 a	67.67 ± 2.78 c	1.54 ± 0.15 a	0.03 ± 0 a	20.54 ± 1 a	0.26 ± 0.02 a

Table 2. Cont.

	%N	%C	%H	%S	%O	(O + N)/C
GORSE	1.55 ± 0.05 A	44.83 ± 1.53 A	6.05 ± 0.11 D	0.08 ± 0.04 A	45.03 ± 1.2 D	0.78 ± 0.05 D
BG300-1H	2.09 ± 0.06 B	58.27 ± 2.09 B	5.42 ± 0.14 C	0.04 ± 0.01 A	31 ± 1.8 C	0.43 ± 0.04 C
BG300-3H	2.48 ± 0.05 C	62.81 ± 1.52 C	4.87 ± 0.11 B	0.04 ± 0.01 A	25.54 ± 1.11 B	0.34 ± 0.02 B
BG600-1H	1.95 ± 0.28 B	71.67 ± 2.03 D	1.72 ± 0.38 A	0.05 ± 0 A	18.81 ± 2.86 A	0.22 ± 0.03 A
BG600-3H	1.63 ± 0.07 A	72.32 ± 2.19 D	1.66 ± 0.14 A	0.05 ± 0 A	19.26 ± 1.97 A	0.22 ± 0.03 A

Finally, the (O + N)/C ratio decreased with pyrolysis temperature and, at 300 °C, with residence time, indicating the loss of nitrogenated and oxygenated functional groups during pyrolysis and the polycondensation reactions that take place during pyrolysis.

Regarding the atomic H/C and O/C ratios, Figure 1 shows the Van Krevelen diagram of the prepared biochars compared to those of different coals. It can be noted that the H/C and O/C ratios of the biochars decreased with pyrolysis temperature. The H/C atomic ratio presented similar values to those obtained by Kaal et al. [53] for gorse-derived biochars.

The Van Krevelen diagram shows some differences between the feedstock (black circle), biochars at 300 °C (discontinuous black circle), and biochars prepared at 600 °C (double-lined black circle). The biochars obtained by pyrolysis at 300 °C presented H/C and O/C ratios close to those of low grade sub-bituminous coals [61] and lignite coal [73]. Instead, biochars at 600 °C presented low H/C and O/C ratios, with H/C values near to those reported for anthracite [74,75], but they had a higher O/C. Therefore, it could be concluded that the biochars from broom and gorse have similar characteristics to those of traditional fossil fuels and eventually could be cleaner substitute energy sources [61].

The biochars from broom and gorse had low S contents (Table 2) compared to those of conventional coals [61,76–78]. Therefore, during the combustion of these biochars, lower SO₂ emissions will be produced, reducing their impact on the environment as well as the costs of purifying the emitted gases.

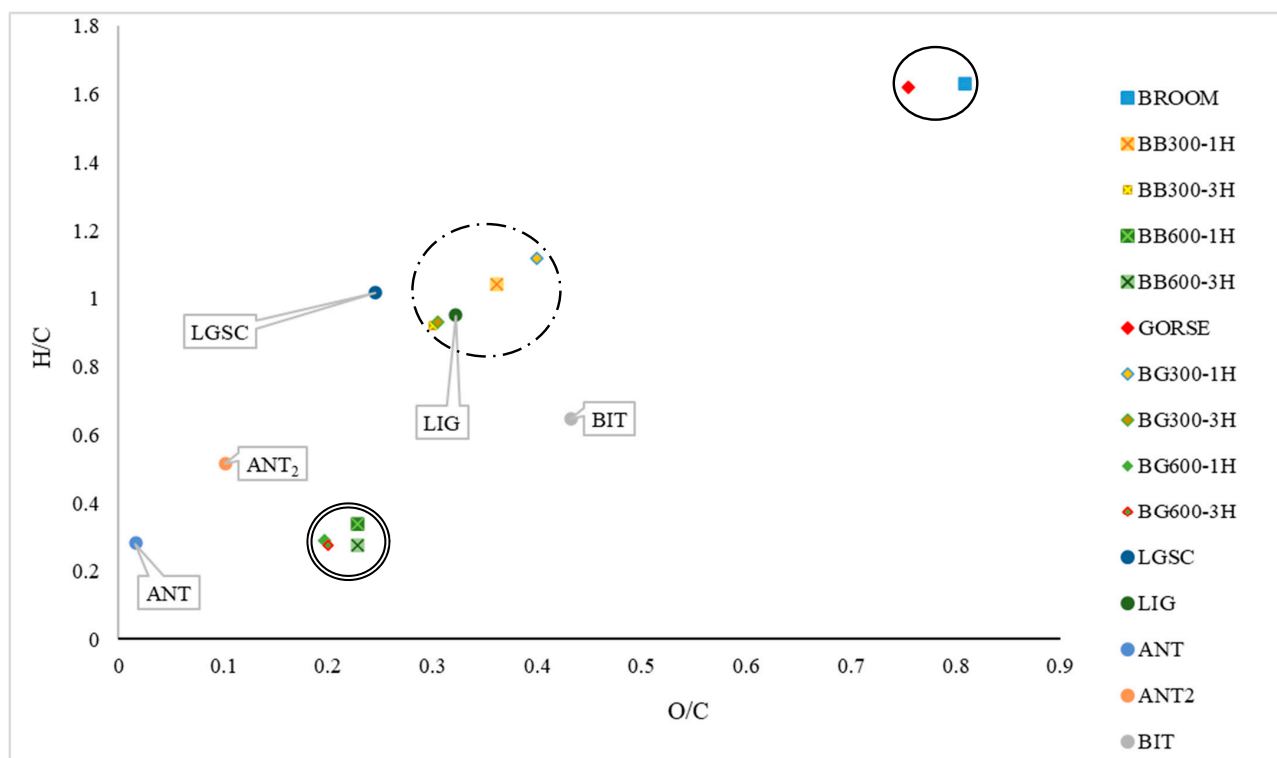


Figure 1. Van Krevelen diagram for broom, gorse, and their biochars. The data with labels correspond to the literature values. LSGC: low-grade sub-bituminous coal [61]; LIG: lignite [73], BIT: bituminous coal [79], ANT: anthracite [75], and ANT2: anthracite [74].

The average HHV of gorse was lower than those found by Núñez-Regueira et al. [54], who obtained values of 20.18 and 20.95 MJ kg⁻¹, and than those measured and calculated by González Martínez et al. [50], with HHV values of 19.5 and 19.6 MJ kg⁻¹ for *U. europaeus*. The average HHV for broom was also lower than that obtained by González Martínez et al. [50] which ranged between 18.6 and 19.3 MJ kg⁻¹ or than those reported by Núñez-Regueira et al. [54] of 19.01 and 20.67 MJ kg⁻¹ for *C. scoparius*.

The average HHV of the feedstock increased with pyrolysis time (Table 3) due to increase in C content [50,58,61]. In addition, the different formulas used for calculating the HHV did not statistically differ among the biochars, except in the case of BB600-1H and BG300-3H. In the broom and gorse feedstocks, there were statistical differences, especially between HHV₁ and HHV₃ for broom and HHV₃ and HHV₄ for gorse (Supporting Information Table S1). The LHV behaviors were the same, with lower values for broom and gorse feedstock compared with those of the biochars. The CDF, linked to energy production, increased with pyrolysis temperature, as has been reported by other authors [60,80,81]. The EEF did not show statistical differences between biochars except in the case of BB300-3H, having a mean value of 1.55 ± 0.07; nevertheless, all biochars presented an EEF greater than one, which, according to Kongto et al. [60], reflects an improvement in energy densification. In terms of calorific value improvement, the CVI did not show differences between the biochars except in the cases of BB300-1H and BB300-3H, which had the highest values.

Table 3. Energy properties of broom, gorse, and their respective biochars. Means with the same letter are not significantly different ($p > 0.05$) according to Duncan's test.

	Average HHV (MJ kg ⁻¹)	LHV (MJ kg ⁻¹)	CDF	EEF	CVI (%)	ED (MJ m ⁻³)
BROOM	15.57 ± 0.25 a	14.28 ± 0.21 a	-	-	-	4359.15 ± 69.41 d
BB300-1H	23.06 ± 1.07 b,c	21.91 ± 1.07 b,c,d	1.4 ± 0.05 b	1.48 ± 0.07 b,c	48.14 ± 6.89 b,c	4151.29 ± 192.96 c,d
BB300-3H	24.18 ± 1.08 c	23.1 ± 1.05 c,d	1.48 ± 0.05 b	1.55 ± 0.07 c	55.3 ± 6.91 c	4351.88 ± 193.64 d
BB600-1H	22.62 ± 0.51 b,c	22.19 ± 0.48 b,c,d	1.62 ± 0.02 c	1.45 ± 0.03 a,b,c	45.31 ± 3.25 a,b,c	5429.27 ± 121.36 e
BB600-3H	21.69 ± 1.33 b	21.35 ± 1.31 b	1.6 ± 0.07 c	1.39 ± 0.09 a,b	39.35 ± 8.55 a,b	5423.48 ± 332.81 e
GORSE	17.02 ± 0.7 a	15.67 ± 0.68 a	-	-	-	3914.25 ± 160.17 b,c
BG300-1H	22.73 ± 0.74 b,c	21.52 ± 0.78 b,c	1.3 ± 0.05 a	1.34 ± 0.04 a	33.56 ± 4.37 a	3636.84 ± 118.99 a,b
BG300-3H	24.21 ± 0.53 c	23.12 ± 0.55 c,d	1.4 ± 0.03 b	1.42 ± 0.03 a,b	42.26 ± 3.09 a,b	3389.41 ± 73.55 a
BG600-1H	23.61 ± 1.46 c	23.22 ± 1.4 c,d	1.6 ± 0.05 c	1.39 ± 0.09 a,b	38.71 ± 8.6 a,b	4013.01 ± 248.95 c,d
BG600-3H	23.71 ± 1.06 c	23.34 ± 1.05 d	1.61 ± 0.05 c	1.39 ± 0.06 a,b	39.34 ± 6.2 a,b	4031.44 ± 179.5 c,d

The ED of broom did not statistically differ between the feedstock and the biochars prepared at 300 °C, but did differ from that obtained at 600 °C. The gorse feedstock and the derived biochars did not differ from the feedstock, except in the case of BG300-3H, which had a lower value. All biochars had ED values greater than those reported for old oil palm trees and the respective biochars [61].

In summary, the energetic characteristics of biochars derived from broom and gorse with pyrolysis at 300 or 600 °C are appropriate materials for fuel and energy production. The HHV and LHV of broom- and gorse-derived biochars are comparable of those obtained in investigations by Kongto et al. [61], who reported an LHV of 18.88 MJ kg⁻¹ and an HHV of 20.04 MJ kg⁻¹ for low-grade sub-bituminous coal and by Cueva Zepeda et al. [82] for conventional fuels like bituminous coal, lignite/brown coal, and coal water slurry, with HHVs of 27.11, 17.33, and 14.03 MJ kg⁻¹ respectively; these values are within the range of variation in the materials in this study (Table 3).

Lignite, a coal similar to the biochars according to the Van Krevelen diagram, had an HHV of between 9.3 and 19.3 MJ kg⁻¹ at 300 °C [63]; meanwhile, for the biochars at 600 °C, the most similar conventional fuel was anthracite (Figure 1). Anthracite has an HHV of 33.58 MJ kg⁻¹ [76] and an LHV of 26.71 MJ kg⁻¹ [77] and 27.47 MJ kg⁻¹ [78]. In this scenario, the biochars had a greater HHV at 300 °C than those reported in the literature

for lignite coal; for biochars at 600 °C, the HHVs were below the HHV and LHV ranges of anthracite. Therefore, all biochars showed HHV values greater than 20 MJ kg⁻¹, which ensures auto-thermal combustion [83].

It could be concluded that the biochars obtained from the pyrolysis of broom and gorse are suitable as fuels, given their adequate energy indices (Table 3). Subsequently, the production of biochars from these biomass waste could provide an adequate valorization technology for cleaner and renewable energy production compared to conventional fossil fuels (i.e., anthracite, lignite, bituminous, or sub-bituminous coal).

3.2. Proximate Analysis

Table 4 summarizes the results of the proximate analysis of broom and gorse and their derived biochars. The VM values were higher for the broom and gorse samples, decreasing with pyrolysis temperature. No differences were found between the residence times at 600 °C but, for the biochars prepared at 300 °C, the VM contents were greater in the biochars pyrolyzed for 1 h than in those obtained after 3 h. There was a marked decrease in the VM content of the biochars pyrolyzed at 600 °C with respect to that of the biochars pyrolyzed at 300 °C. All biochars had a low ash content, which was related to the low values in the two feedstocks. The ash content of broom and gorse in another investigation was lower than 1% [54]. In the broom-derived biochars, the highest ash content was found for BB600-3H, and, in gorse-based biochars, it was in BG600-1H. In all cases, the ash content was lower than that of coal fuels [77,78]. The FC content increased with pyrolysis temperature, and, at 600 °C, no statistical differences were found between the residence times for the broom- and gorse-derived biochars, but the FC contents were above 80% in these high-temperature-pyrolyzed biochars compares to those of the biochars pyrolyzed at 300 °C.

Table 4. Proximate analyses (dry basis) for broom, gorse, and the respective biochars. Means with the same letter are not significantly different ($p > 0.05$) using Duncan test for broom (lower case letters) and gorse (upper case letters) independently.

	VM (%)	Ash (%)	FC (%)	FC/VM	FC/(VM + FC)
BROOM	80.71 ± 0.29 d	3.16 ± 1.03 a	16.12 ± 1.32 a	0.2 ± 0.02 a	0.17 ± 0.01 a
BB300-1H	56.32 ± 2.41 c	3.91 ± 0.73 a,b	39.78 ± 3.11 b	0.71 ± 0.09 a,b	0.41 ± 0.03 b
BB300-3H	47.38 ± 0.73 b	4.33 ± 0.8 a,b	48.29 ± 1.33 c	1.02 ± 0.04 b	0.5 ± 0.01 c
BB600-1H	13.47 ± 0.82 a	5.89 ± 1.64 b,c	80.64 ± 2.46 d	6.01 ± 0.57 c	0.86 ± 0.01 d
BB600-3H	12.03 ± 0.81 a	7.58 ± 1.73 c	80.39 ± 2.54 d	6.71 ± 0.69 c	0.87 ± 0.01 d
GORSE	82.94 ± 0.9 D	2.47 ± 0.47 A	14.6 ± 1.16 A	0.18 ± 0.02 A	0.15 ± 0.01 A
BG300-1H	60.05 ± 1.76 C	3.17 ± 0.21 B	36.77 ± 1.97 B	0.61 ± 0.05 A	0.38 ± 0.02 B
BG300-3H	48.01 ± 2.42 B	4.26 ± 0.36 C	47.73 ± 2.78 C	1 ± 0.11 A	0.5 ± 0.03 C
BG600-1H	12.82 ± 1.84 A	5.8 ± 0.32 E	81.37 ± 1.52 D	6.45 ± 1.14 B	0.86 ± 0.02 D
BG600-3H	10.3 ± 0.51 A	5.09 ± 0.32 D	84.61 ± 0.8 D	8.23 ± 0.5 C	0.89 ± 0.01 D

The FC content increased with the increase in temperature due to the combination of processes that happen during pyrolysis: (i) polycondensation, (ii) aromatization, and (iii) defunctionalization of the matrix [84]. This occurred according to the evolution of the other properties with pyrolysis temperature (Table 2 and Figure 1). The biochars prepared at 600 °C had a high FC content; in all cases, it was possible to produce more heat with a longer combustion, which was proportional to the energy content [61].

The FC/VM values (Table 4), known as the fuel ratio, were greater for biochars prepared at 600 °C [63]. This result is consistent with the evolution of the H/C and O/C ratios as well as the FC content.

The thermal stability, in accordance with the FC/(VM + FC) index, was highest for BB600 and BG600 at 1 h and 3 h and the lowest for the feedstock. The FC/VM and the FC/(VM + FC) had the same behavior. This means that biochars pyrolyzed at 600 °C were more stable owing to the larger number of aromatic carbon structures. The more-labile

carbon structures were linked to biochars prepared at 300 °C and were related to the VM contents, which were higher in these biochars (Table 4). Therefore, the H/C molar ratio is related to biochar aromaticity and thermal stability [71].

3.3. Chemical Properties

Regarding C_{oxi} , which represents the labile fraction of carbon and consequently, works as an indicator of the degree of biomass carbonization, the results showed a decrease with pyrolysis temperature. The biochars obtained at 600 °C (BB600 and BG600) had the low C_{oxi} values, indicating high chemical stability (Table 5). For WEOC, the following trend was found: broom > BB300-1H > BB300-3H = BB600-1H = BB600-3H and gorse > BG300-1H > BG300-3H > BG6001H = BG600-3H (Table 5). The WEOC decreased with the pyrolysis temperature and was related to the stability and the presence of more aromatic carbon structures. A previous investigation reported the presence of more aromatic carbon structures in biochars at 600, which resist water extraction [3].

Table 5. C_{oxi} , pH, EC, and WEOC (dry basis) for broom, gorse, and their respective biochars. Means with the same letter are not significantly different ($p > 0.05$) according to Duncan's test for broom (lower case) and gorse (upper case) independently.

	C_{oxi} (%)	pH	EC ($\mu\text{S cm}^{-1}$)	WEOC (mg kg^{-1})
BROOM	44.36 ± 0.76 c	5.65 ± 0.04 a	218.67 ± 18.01 c	67,196.37 ± 1882.12 c
BB300-1H	45.78 ± 0.82 c	8.56 ± 0.31 b	95 ± 3.96 b	4671.04 ± 131.73 b
BB300-3H	39.12 ± 1.09 b	8.90 ± 0.19 c	75.27 ± 2.74 a	1086.64 ± 9.68 a
BB600-1H	1.31 ± 0.9 a	9.53 ± 0.15 d	215.33 ± 2.52 c	777.77 ± 22.35 a
BB600-3H	2.17 ± 0.44 a	9.52 ± 0.11 d	263 ± 8.54 d	1001.02 ± 44.59 a
GORSE	42.95 ± 1.21 B	6.48 ± 0.14 A	108.8 ± 1.7 B	31,396.85 ± 187.82 D
BG300-1H	47.24 ± 1.32 C	8.28 ± 0.03 B	104.25 ± 2.95 A,B	3619.17 ± 44.23 C
BG300-3H	41.2 ± 1.79 B	9.59 ± 0.17 C	100.23 ± 1.69 A	735.52 ± 15.29 B
BG600-1H	5.88 ± 0.35 A	10.42 ± 0.12 D	233.67 ± 4.16 D	510.38 ± 19.54 A
BG600-3H	6.32 ± 0.19 A	10.32 ± 0.04 D	209.5 ± 4.5 C	449.66 ± 20.86 A

The pH presented a well-studied pattern for biochars [85], values with pyrolysis temperature (Table 5). The biochars had low EC values ($<300 \mu\text{S cm}^{-1}$), with the highest values found for the biochars obtained at the highest temperature. The high pH values of the biochars were due to several factors: (i) the separation of alkali salts from organic materials [13], (ii) the increase in carbonate content [85], (iii) the loss of carboxylic groups with the rise in pyrolysis temperature, (iv) the increase in the number of functional oxygen groups [86], and (v) the increase in ash content [86]. The residence time did not change the pH values at 600 °C. At this temperature, the material was more stable. For the biochars produced at 300 °C, the lower pH values at 1 h than at 3 h were due to the carbonization reactions, which need more time to occur. The EC results suggested some salt formation and concentration with pyrolysis, leading to a high EC for biochars produced at 600 °C. In addition, the breakdown of some organic structures with pyrolysis led to an increase in their solubilization [87,88].

3.4. Physical Properties

Table 6 summarizes the physical properties of the biochars. The porosity increased with pyrolysis duration for both the broom- and gorse-derived biochars. The highest porosity for broom-derived biochars was recorded for BB600-3H and for BG600-1H for gorse-derived biochars. The V mesoporosity increased in the broom-derived biochars with pyrolysis temperature. On the contrary, the V mesoporosity in gorse-derived biochars produced at 300 °C was lower than that of the feedstock but higher than that of the biochars produced at 600 °C. The V macroporosity was higher in biochars than in the feedstock (broom and gorse).

Table 6. Physical properties (dry basis) of broom, gorse, and their respective biochars.

	Measured Porosity (%)	V _{meso} (cm ³ g ⁻¹)	V _{macro} (cm ³ g ⁻¹)	Bulk Density (g cm ⁻³)	Solid Density (g cm ⁻³)	Calculated Total Porosity (%)
BROOM	43.59	0.06	0.51	0.28	1.28	78.12
BB300-1H	56.51	0.08	0.97	0.18	1.28	85.68
BB300-3H	57.59	0.09	1.04	0.18	1.27	85.50
BB600-1H	57.80	0.18	0.88	0.24	1.47	83.45
BB600-3H	60.28	0.19	1.04	0.25	1.53	83.93
GORSE	34.69	0.12	0.24	0.23	1.34	82.91
BG300-1H	52.15	0.07	0.77	0.16	1.29	87.73
BG300-3H	48.06	0.07	0.79	0.14	1.36	89.61
BG600-1H	57.14	0.13	0.93	0.17	1.47	88.72
BG600-3H	56.79	0.19	0.86	0.17	1.49	88.73

The bulk density presented the highest values for broom and gorse feedstock; instead, the solid density was the highest for the biochars fabricated at 600 °C. These data are consistent with the presence of more pores at low pyrolysis temperatures than in solids. The total porosity of the broom materials support the aforementioned behavior, with higher values found for the biochars produced at 300 °C. For the gorse-derived materials, the total porosities for all biochars were similar but higher than those of the gorse.

Vaughn et al. [89] reported a similar solid density for species of the Fabaceae family, specifically, black locust, eastern redbud, and honey locust, with values of 1.57, 1.72, and 1.82 g cm⁻³, respectively. Another investigation of woody biomass reported a bulk density of 0.73 g cm⁻³ and specific gravity density of 1.36 g cm⁻³ [90]. Those data are comparable to the present results (Table 6), with our values being within the ranges. Regarding the porosity and V mesoporosity, the trends were the same as those in other investigations [91], where the increase in pyrolysis temperature led to a more developed pore structure.

3.5. PAH Content

The PAH contents were measured in order to evaluate the potential environmental risk of BC, taking to account that these organic compounds can affect plant and human health [92]. In the case of light PAHs, the greatest contribution was from acenaphthene and fluorene for all biochars (Supporting Information Table S2). The naphthalene and acenaphthylene contents were low; in some cases, no amount was detected. The concentrations of light PAHs were low and did not exceed the 3.5 ng g⁻¹ (Supporting Information Table S2). For medium PAHs, the greatest amount belonged to phenanthrene, which had a maximum value of 24.07 ng g⁻¹ in BB300-3H. The amounts of anthracene and fluoranthene were lower in the medium PAHs (Supporting Information Table S2). In the case of heavy PAHs, no specific PAH was a major contributor, except in the case of dibenzo [a,h] anthracene in BG300-1H and BG300-3H (Supporting Information Table S2).

In general, the PAH contents were low and between the ranges of the acceptable limits for biochar materials according to the European Biochar Certificate guidelines [93]. In addition, greater concentrations have been detected for other biochar materials [3,92]. Schleder et al. [94] stated that pyrolysis influences the PAH concentration, where low-temperature biochars have a greater PAH concentration. In this case, the trend was the same for gorse-derived biochars (Figure 2), with greater values found for total PAHs (Σ light, medium, and heavy) in BG300-1H, followed by BG300-3H. In the broom-derived biochars, the highest value was found for BB300-3H.

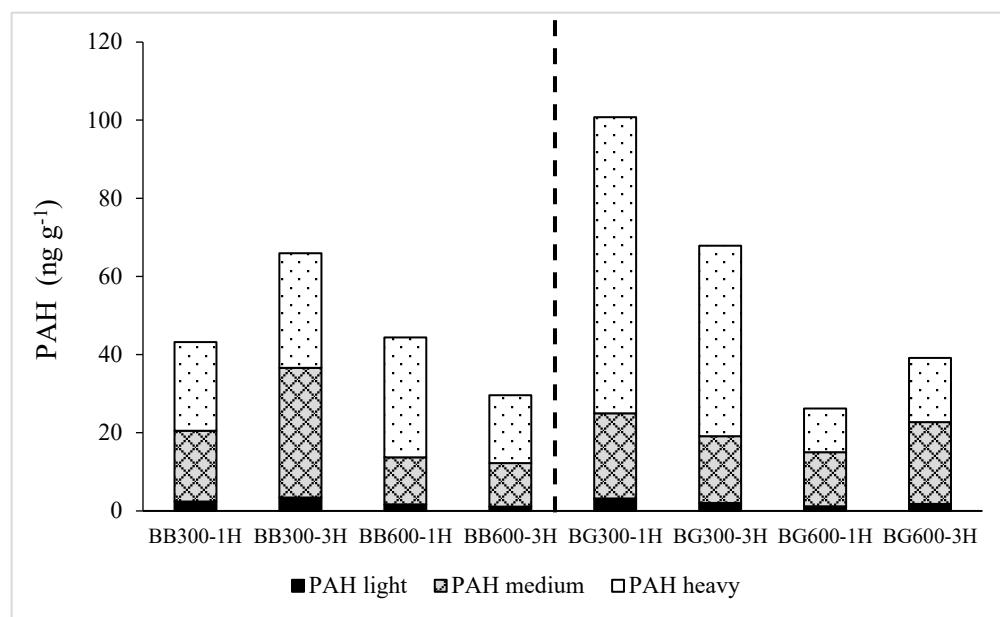


Figure 2. PAH contents (ng g^{-1}) for broom, gorse, and their respective biochars.

3.6. Statistical Analysis

After an extensive analysis of the gorse and broom feedstock and the biochars, some interactions were assessed in order to understand the synergic effect of the pyrolysis conditions and the feedstock on the properties of the particular biochars. The Pearson product-moment correlation analysis (Supporting Information, Table S3) and PCA (Supporting Information, Figure S1) were performed using elemental composition parameters, HHV, and proximate analysis parameters. The results showed that the amount of C was the key variable determining the HHV and the related energy indices. The HHV positively correlated ($r = 0.86$) with C, while it negatively correlated with H, O, H/C, O/C, and $(O + H)/C$. Moreover, HHV was positively related to FC and ash content and negatively related to VM.

The first and second PCs explained 78.8% and 10.9% of the variation, respectively, while these two PCs accounted for 86.7% of the total variation. The distributions of feedstocks and biochars produced at 300 °C and 600 °C, resulting from the plot of PC1 versus PC2 scores, are shown in Figure S2 in the Supporting Information. The figure provides a precise visualization of the separation between the studied datasets. Consistent with previous results, we found that pyrolysis temperature was the main factor influencing sample distribution, and not feedstock type or residence time.

Table 7 shows the results of the ANOVA. The elemental analysis, proximate analysis, energy properties, and C_{oxi} did not show an interactions between the residence time and the feedstock. For the abovementioned properties, the major interactions were found between pyrolysis temperature and residence time. No interactions were registered between feedstock: temperature: residence time, except for the ED, pH, EC, and WEOC (Table 7). Properties like %H, %S, ash, HHV average, EEF, and CVI did not show any interactions.

The temperature was a key factor affecting the biochar properties, and the residence time was less important. Variation in the feedstock did not seem to have an effect; this result could have been due to the nature of the species: gorse and broom are species of the same family with similar characteristics, and both of them have a high fuel value.

The analyses of the feedstock and biochars indicate a suitable valorization strategy. Galicia and north Portugal are areas well known for several fires each year [34]. Species like broom and gorse represent a fire risk in this area due to (i) covering vast areas of scrubland and forest [55], (ii) spreading rapidly, (iii) their susceptibility to fire [27], and (iv) increasing the frequency, intensity, and severity of fires [95].

Table 7. Interactions between biochar properties and the pyrolysis parameters (temperature and residence time) and the feedstock. x represents a synergic effect ($p < 0.05$) determined using 3-way ANOVA, and - indicates no synergic effect.

Interactions	Feedstock:Residence Time		Temperature:Residence Time		Feedstock:Temperature		Feedstock:Temperature:Residence Time
	300 °C	600 °C	Broom	Gorse	1 h	3 h	
N	-	-	x	x	-	-	-
C	-	-	x	x	x	x	-
H	-	-	-	-	-	-	-
S	-	-	-	-	-	-	-
O	-	-	x	x	x	x	-
H/C	-	-	x	x	-	-	-
O/C	-	-	x	x	x	x	-
(O + N)/C	-	-	x	x	x	x	-
HHV _{average}	-	-	-	-	-	-	-
LHV	-	-	x	x	-	-	-
CDF	-	-	x	x	x	x	-
EEF	-	-	-	-	-	-	-
CVI	-	-	-	-	-	-	-
ED	-	-	-	-	x	x	x
VM	-	-	x	x	x	x	-
Ash	-	-	-	-	-	-	-
FC	-	-	x	x	x	x	-
FC/VM	-	-	-	-	x	x	-
FC/(VM + FC)	-	-	x	x	x	x	-
Coxi	-	-	x	x	x	x	-
pH	x	x	x	x	x	x	x
EC	x	x	x	x	x	x	x
WEOC	x	x	x	x	x	x	x

Gorse has been used as animal bedding for livestock, compost to fertilize fields, and waste [30], but, at the present time, these shrublands have been mostly abandoned [53], generating unused biomass. Broom has been less studied and used in Galicia than gorse, but some investigations in North America indicated Scotch broom as an important competitor for commercial crop trees [19].

Broom and gorse shrublands have been mostly abandoned, and this biomass remains unemployed. As such, the biochars derived from these feedstocks are suitable as an energy source. From extensive characterization, broom and gorse biochars presented appropriate properties for use as fuels for energy production. From an environmental point of view, they pose no risk related to PAH content. However, future investigations are needed to better understand the use of broom and gorse biochars in energy production; as these biochars are rich in carbon, low in ash, they may be used as carbon-reducing materials in different processes based on carbothermic reduction reactions.

4. Conclusions

Broom and gorse biomass, which is abundant worldwide either as native or introduced shrubs, can be used as feedstock for the production of biochars. The main study conclusions are as follows:

Broom- and gorse-derived biochars have a high carbon content and are stable, with high calorific values and appropriate energy properties, so they are suitable as renewable fuels for green energy production or as carbon-reducing materials.

The use of broom- and gorse-derived biochars is safe in terms of environmental risk given their low PAH contents.

Finally, regarding pyrolysis conditions, in general, the residence time did not seem to influence biochar properties, especially those of biochars produced at high temperatures.

The variation in the feedstock did not seem to have an effect on most of the properties; this result could be due to the nature of the species: gorse and broom are legumes with similar characteristics.

Supplementary Materials: The following supporting information can be downloaded at: <https://www.mdpi.com/article/10.3390/app14104283/s1>. Table S1: Four HHV for broom, gorse and the respective biochars. Means with the same letter are not significantly different ($p > 0.05$) using Duncan test for broom and gorse independently (lowercase letter). The capital letters represents the difference between the HHV calculated for each sample. Table S2: PAHs (ng g^{-1}) for broom and gorse and the respective biochars. Table S3: Correlation matrix for elemental analysis parameters (N, C, H, O, H/C, O/C, (O+N)/C, H), HHV, and proximate analysis parameters (VM, FC and ash content). Figure S1: PCA loading plots for elemental analysis parameters (N, C, H, O, H/C, O/C, (O+N)/C), HHV, and proximate analysis parameters (VM, FC and ash content). Figure S2: PC1 versus PC2 score-score plot showing the distributions for broom and gorse and the respective biochars.

Author Contributions: Conceptualization, E.C.-A., A.M. and A.P.-G.; methodology, E.C.-A.; software, M.L.; validation, A.M., G.G. and M.L.; formal analysis, E.C.-A., A.M., G.G., M.L. and A.P.-G.; investigation, E.C.-A., A.M., G.G., M.L. and A.P.-G.; resources, E.C.-A. and A.P.-G.; data curation, E.C.-A.; writing—original draft preparation, E.C.-A., A.M. and A.P.-G.; writing—review, E.C.-A., A.M., G.G., M.L. and A.P.-G.; editing, E.C.-A.; supervision, A.M., G.G., M.L. and A.P.-G.; project administration, A.P.-G.; funding acquisition, E.C.-A. and A.P.-G. All authors have read and agreed to the published version of the manuscript.

Funding: This research was funded by Unión Europea-NextGenerationEU [grant number UP2021-035, 2022], Ministerio de Universidades, and Universidad Politécnica de Madrid.

Institutional Review Board Statement: Not applicable.

Informed Consent Statement: Not applicable.

Data Availability Statement: The raw data supporting the conclusions of this article will be made available by the authors on request.

Conflicts of Interest: The authors declare no conflicts of interest.

References

1. Lehmann, J.; Rillig, M.C.; Thies, J.; Masiello, C.A.; Hockaday, W.C.; Crowley, D. Biochar Effects on Soil Biota—A Review. *Soil Biol. Biochem.* **2011**, *43*, 1812–1836. [[CrossRef](#)]
2. Wang, S.; Zhang, H.; Huang, H.; Xiao, R.; Li, R.; Zhang, Z. Influence of Temperature and Residence Time on Characteristics of Biochars Derived from Agricultural Residues: A Comprehensive Evaluation. *Process Saf. Environ. Prot.* **2020**, *139*, 218–229. [[CrossRef](#)]
3. Cárdenas-Aguiar, E.; Gascó, G.; Lado, M.; Méndez, A.; Paz-Ferreiro, J.; Paz-González, A. New Insights into the Production, Characterization and Potential Uses of Vineyard Pruning Waste Biochars. *Waste Manag.* **2023**, *171*, 452–462. [[CrossRef](#)] [[PubMed](#)]
4. Méndez, A.; Tarquis, A.M.; Saa-Requejo, A.; Guerrero, F.; Gascó, G. Influence of Pyrolysis Temperature on Composted Sewage Sludge Biochar Priming Effect in a Loamy Soil. *Chemosphere* **2013**, *93*, 668–676. [[CrossRef](#)]
5. Gascó, G.; Paz-Ferreiro, J.; Álvarez, M.L.; Saa, A.; Méndez, A. Biochars and Hydrochars Prepared by Pyrolysis and Hydrothermal Carbonisation of Pig Manure. *Waste Manag.* **2018**, *79*, 395–403. [[CrossRef](#)] [[PubMed](#)]
6. Álvarez, M.L.; Méndez, A.; Paz-Ferreiro, J.; Gascó, G. Effects of Manure Waste Biochars in Mining Soils. *Appl. Sci.* **2020**, *10*, 3393. [[CrossRef](#)]
7. Cárdenas-Aguiar, E.; Méndez, A.; Paz-Ferreiro, J.; Gascó, G. The Effects of Rabbit Manure-Derived Biochar on Soil Health and Quality Attributes of Two Mine Tailings. *Sustainability* **2022**, *14*, 866. [[CrossRef](#)]
8. Méndez, a.; Paz-Ferreiro, J.; Araujo, F.; Gascó, G. Biochar from Pyrolysis of Deinking Paper Sludge and Its Use in the Treatment of a Nickel Polluted Soil. *J. Anal. Appl. Pyrolysis* **2014**, *107*, 46–52. [[CrossRef](#)]
9. Liang, C.; Gascó, G.; Fu, S.; Méndez, A.; Paz-Ferreiro, J. Biochar from Pruning Residues as a Soil Amendment: Effects of Pyrolysis Temperature and Particle Size. *Soil Tillage Res.* **2016**, *164*, 3–10. [[CrossRef](#)]
10. Sánchez-García, M.; Cayuela, M.L.; Rasse, D.P.; Sánchez-Monedero, M.A. Biochars from Mediterranean Agroindustry Residues: Physicochemical Properties Relevant for C Sequestration and Soil Water Retention. *ACS Sustain. Chem. Eng.* **2019**, *7*, 4724–4733. [[CrossRef](#)]
11. Mukherjee, A.; Patra, B.R.; Podder, J.; Dalai, A.K. Synthesis of Biochar From Lignocellulosic Biomass for Diverse Industrial Applications and Energy Harvesting: Effects of Pyrolysis Conditions on the Physicochemical Properties of Biochar. *Front. Mater.* **2022**, *9*, 870184. [[CrossRef](#)]

12. Liu, W.J.; Yu, H.Q. Thermochemical Conversion of Lignocellulosic Biomass into Mass-Produced Fuels: Emerging Technology Progress and Environmental Sustainability Evaluation. *ACS Environ. Au* **2022**, *2*, 98–114. [[CrossRef](#)] [[PubMed](#)]
13. Tomczyk, A.; Sokołowska, Z.; Boguta, P. Biochar Physicochemical Properties: Pyrolysis Temperature and Feedstock Kind Effects. *Rev. Environ. Sci. Biotechnol.* **2020**, *19*, 191–215. [[CrossRef](#)]
14. Benavente, I.; Gascó, G.; Plaza, C.; Paz-Ferreiro, J.; Méndez, A. Choice of Pyrolysis Parameters for Urban Wastes Affects Soil Enzymes and Plant Germination in a Mediterranean Soil. *Sci. Total Environ.* **2018**, *634*, 1308–1314. [[CrossRef](#)] [[PubMed](#)]
15. Zwölfer, H. *Ulex Europaeus Project; European Investigations for New Zealand*; Commonwealth Insistitue of Biological Control: Delémont, Switzerland, 1962.
16. Brandes, U.; Furevik, B.B.; Nielsen, L.R.; Kjær, E.D.; Rosef, L.; Fjellheim, S. Introduction History and Population Genetics of Intracontinental Scotch Broom (*Cytisus scoparius*) Invasion. *Divers. Distrib.* **2019**, *25*, 1773–1786. [[CrossRef](#)]
17. Heywood, V.H.; Ball, P.W. Leguminosae. In *Flora Europaea: Rosaceae to Umbelliferae*; Tutin, Thomas Gaskell, 1908th ed.; Cambridge University Press: Great Britain, UK, 1968; Volume 2, p. 489. ISBN 0521 06662 X.
18. Williams, P.A. Aspects of the Ecology of Broom (*Cytisus scoparius*) in Canterbury, New Zealand. *N. Zeal. J. Bot.* **1981**, *19*, 31–43. [[CrossRef](#)]
19. Peterson, D.J.; Prasad, R. The Biology of Canadian Weeds. 109. *Cytisus scoparius* (L.) Link. *Can. J. Plant Sci.* **1998**, *78*, 497–504. [[CrossRef](#)]
20. Broadfield, N.; McHenry, M.T. A World of Gorse: Persistence of *Ulex Europaeus* in Managed Landscapes. *Plants* **2019**, *8*, 523. [[CrossRef](#)] [[PubMed](#)]
21. Galappaththi, H.S.S.D.; de Silva, W.A.P.P.; Clavijo McCormick, A. A Mini-Review on the Impact of Common Gorse in Its Introduced Ranges. *Trop. Ecol.* **2023**, *64*, 1–25. [[CrossRef](#)]
22. Rojas-Sandoval, J. CABI International, *Ulex Europaeus* (Gorse). Available online: <https://www.cabidigitallibrary.org/doi/10.1079/cabicompendium.55561> (accessed on 20 March 2024).
23. Rojas-Sandoval, J. CABI International, *Cytisus scoparius* (Scotch Broom). Available online: <https://www.cabidigitallibrary.org/doi/10.1079/cabicompendium.17610> (accessed on 20 March 2024).
24. León Cordero, R.; Torchelsen, F.P.; Overbeck, G.E.; Anand, M. Invasive Gorse (*Ulex Europaeus*, Fabaceae) Changes Plant Community Structure in Subtropical Forest–Grassland Mosaics of Southern Brazil. *Biol. Invasions* **2016**, *18*, 1629–1643. [[CrossRef](#)]
25. Cordero, R.L.; Torchelsen, F.P.; Overbeck, G.E.; Anand, M. *Cytisus scoparius* (Fam. Fabaceae) in Southern Brazil—First Step of an Invasion Process? *An. Acad. Bras. Cienc.* **2016**, *88*, 149–154. [[CrossRef](#)] [[PubMed](#)]
26. Bateman, J.B.; Vitousek, P.M. Soil Fertility Response to *Ulex Europaeus* Invasion and Restoration Efforts. *Biol. Invasions* **2018**, *20*, 2777–2791. [[CrossRef](#)]
27. Udo, N.; Darrot, C.; Atlan, A. From Useful to Invasive, the Status of Gorse on Reunion Island. *J. Environ. Manag.* **2019**, *229*, 166–173. [[CrossRef](#)] [[PubMed](#)]
28. DAISIE Handbook of Alien Species in Europe. In *Invading Nature—Springer Series in Invasion Ecology*; Springer: Knoxville, TN, USA, 2009; ISBN 978-1-4020-8279-5.
29. Pardo-Muras, M.; Puig, C.G.; Souza-Alonso, P.; Pedrol, N. The Phytotoxic Potential of the Flowering Foliage of Gorse (*Ulex Europaeus*) and Scotch Broom (*Cytisus scoparius*), as Pre-Emergent Weed Control in Maize in a Glasshouse Pot Experiment. *Plants* **2020**, *9*, 203. [[CrossRef](#)] [[PubMed](#)]
30. Bada, L.; Pereira, R.B.; Pereira, D.M.; Lores, M.; Celeiro, M.; Quezada, E.; Uriarte, E.; Gil-Longo, J.; Viña, D. Phytochemical Analysis and Antiproliferative Activity of *Ulex Gallii* Planch. (Fabaceae), a Medicinal Plant from Galicia (Spain). *Molecules* **2023**, *28*, 351. [[CrossRef](#)] [[PubMed](#)]
31. USDA-NRCS The PLANTS Database. Available online: <http://plants.usda.gov/> (accessed on 21 March 2024).
32. Donegal County Council (DCC) Gorse Fires. Available online: <https://www.donegalcoco.ie/services/fireservice/gorsefires/> (accessed on 20 March 2024).
33. Gorse Action Group (GAG) Gorse and Fire Risk. Available online: <https://gorseactiongroup.org/gorse-fire-risk/> (accessed on 20 March 2024).
34. Marino, E.; Guijarro, M.; Hernando, C.; Madrigal, J.; Díez, C. Fire Hazard after Prescribed Burning in a Gorse Shrubland: Implications for Fuel Management. *J. Environ. Manag.* **2011**, *92*, 1003–1011. [[CrossRef](#)] [[PubMed](#)]
35. Vega, J.A.; Arellano-Pérez, S.; Álvarez-González, J.G.; Fernández, C.; Jiménez, E.; Fernández-Alonso, J.M.; Vega-Nieva, D.J.; Briones-Herrera, C.; Alonso-Rego, C.; Fontúrbel, T.; et al. Modelling Aboveground Biomass and Fuel Load Components at Stand Level in Shrub Communities in NW Spain. *For. Ecol. Manag.* **2022**, *505*, 119926. [[CrossRef](#)]
36. Vega, J.A.; Álvarez-González, J.G.; Arellano-Pérez, S.; Fernández, C.; Cuiñas, P.; Jiménez, E.; Fernández-Alonso, J.M.; Fontúrbel, T.; Alonso-Rego, C.; Ruiz-González, A.D. Developing Customized Fuel Models for Shrub and Bracken Communities in Galicia (NW Spain). *J. Environ. Manag.* **2024**, *351*, 119831. [[CrossRef](#)] [[PubMed](#)]
37. de Galicia, X. Cosellería do Medio Rural, Dirección Xeral de Ordenación Producción Forestal, C. do M.R. *Primeira Revisión Do Plan Forestal de Galicia*; 2021. Available online: <https://www.ptfor.es/2022/12/22/http-www-ptfor-es-wp-content-uploads-sites-10-2022-12-20211112-plan-forestal-galicia-2021-2040-cast-1-pdf/> (accessed on 14 May 2024).
38. Chaves Fernandes, B.C.; Ferreira Mendes, K.; Dias Júnior, A.; da Silva Caldeira, V.; da Silva Teófilo, T.; Severo Silva, T.; Mendonça, V.; de Freitas Souza, M.; Valadão Silva, D. Impact of Pyrolysis Temperature on the Properties of Eucalyptus Wood-Derived Biochar. *Materials* **2020**, *13*, 5841. [[CrossRef](#)]

39. Francis, J.C.; Nighojkar, A.; Kandasubramanian, B. Relevance of Wood Biochar on CO₂ Adsorption: A Review. *Hybrid Adv.* **2023**, *3*, 100056. [[CrossRef](#)]
40. Zhao, Y.; Feng, D.; Zhang, Y.; Tang, W.; Meng, S.; Guo, Y.; Sun, S. Migration of Alkali and Alkaline Earth Metallic Species and Structure Analysis of Sawdust Pyrolysis Biochar. *Korean Chem. Eng. Res.* **2016**, *54*, 659–664. [[CrossRef](#)]
41. Feng, Q.; Wang, B.; Chen, M.; Wu, P.; Lee, X.; Xing, Y. Invasive Plants as Potential Sustainable Feedstocks for Biochar Production and Multiple Applications: A Review. *Resour. Conserv. Recycl.* **2021**, *164*, 105204. [[CrossRef](#)]
42. Yousaf, B.; Liu, G.; Abbas, Q.; Ali, M.U.; Wang, R.; Ahmed, R.; Wang, C.; Al-Wabel, M.I.; Usman, A.R.A. Operational Control on Environmental Safety of Potentially Toxic Elements during Thermal Conversion of Metal-Accumulator Invasive Ragweed to Biochar. *J. Clean. Prod.* **2018**, *195*, 458–469. [[CrossRef](#)]
43. Fan, L.; Zhou, X.; Liu, Q.; Wan, Y.; Cai, J.; Chen, W.; Chen, F.; Ji, L.; Cheng, L.; Luo, H. Properties of Eupatorium Adenophora Spreng (Crofton Weed) Biochar Produced at Different Pyrolysis Temperatures. *Environ. Eng. Sci.* **2019**, *36*, 937–946. [[CrossRef](#)]
44. Ahmad, M.; Moon, D.H.; Vithanage, M.; Koutsospyros, A.; Lee, S.S.; Yang, J.E.; Lee, S.E.; Choong, J.; Ok, Y.S. Production and Use of Biochar from Buffalo-Weed (*Ambrosia Trifida* L.) for Trichloroethylene Removal from Water. *J. Chem. Technol. Biotechnol.* **2013**, *89*, 150–157. [[CrossRef](#)]
45. Feng, J.; Zhu, Y. Alien Invasive Plants in China: Risk Assessment and Spatial Patterns. *Biodivers. Conserv.* **2010**, *19*, 3489–3497. [[CrossRef](#)]
46. Núñez-Regueira, L.; Proupín-Castiñeiras, J.; Rodríguez-Añón, J.A. Energy Evaluation of Forest Residues Originated from Shrub Species in Galicia. *Bioresour. Technol.* **2004**, *91*, 215–221. [[CrossRef](#)] [[PubMed](#)]
47. Soliño, M.; Prada, A.; Vázquez, M.X. Designing a Forest-Energy Policy to Reduce Forest Fires in Galicia (Spain): A Contingent Valuation Application. *J. For. Econ.* **2010**, *16*, 217–233. [[CrossRef](#)]
48. Amutio, M.; Lopez, G.; Alvarez, J.; Moreira, R.; Duarte, G.; Nunes, J.; Olazar, M.; Bilbao, J. Flash Pyrolysis of Forestry Residues from the Portuguese Central Inland Region within the Framework of the BioREFINA-Ter Project. *Bioresour. Technol.* **2013**, *129*, 512–518. [[CrossRef](#)]
49. Beltrán, V.; Martínez, L.V.; López, A.; Gómez, M.F. Kinetic Analysis of Wood Residues and Gorse (*Ulex Europaeus*) Pyrolysis under Non-Isothermal Conditions: A Case of Study in Bogotá, Colombia. *E3S Web Conf.* **2019**, *103*, 02004. [[CrossRef](#)]
50. González Martínez, M.; Dupont, C.; da Silva Perez, D.; Míguez-Rodríguez, L.; Grateau, M.; Thiéry, S.; Tamminen, T.; Meyer, X.M.; Gourdon, C. Assessing the Suitability of Recovering Shrub Biowaste Involved in Wildland Fires in the South of Europe through Torrefaction Mobile Units. *J. Environ. Manag.* **2019**, *236*, 551–560. [[CrossRef](#)] [[PubMed](#)]
51. Gómez, K.Y.; Quevedo, N.R.; Molina, L.D.C. Use of the Biochar Obtained by Slow Pyrolysis from *Ulex Europaeus* in the Removal of Total Chromium from the Bogotá-Colombia River Water. *Chem. Eng. Trans.* **2021**, *86*, 289–294. [[CrossRef](#)]
52. Page-Dumroese, D.S.; Coleman, M.D.; Thomas, S.C. Opportunities and Uses of Biochar on Forest Sites in North America. In *Biochar: A Regional Supply Chain Approach in View of Mitigating Climate Change*; Cambridge University Press: Cambridge, UK, 2016; pp. 315–335.
53. Kaal, J.; Martínez Cortizas, A.; Reyes, O.; Soliño, M. Molecular Characterization of *Ulex Europaeus* Biochar Obtained from Laboratory Heat Treatment Experiments—A Pyrolysis-GC/MS Study. *J. Anal. Appl. Pyrolysis* **2012**, *95*, 205–212. [[CrossRef](#)]
54. Núñez-Regueira, L.; Rodríguez Añón, J.A.; Proupín Castiñeiras, J. Calorific Values and Flammability of Forest Species in Galicia. Coastal and Hillside Zones. *Bioresour. Technol.* **1996**, *57*, 283–289. [[CrossRef](#)]
55. Puentes, A.; Basanta, M. Architecture of *Ulex Europaeus*: Changes in the Vertical Distribution of Organs in Relation to Plant Height and Season. *J. Veg. Sci.* **2002**, *13*, 793–802. [[CrossRef](#)]
56. Cárdenas-Aguar, E.; Gascó, G.; Paz-Ferreiro, J.; Méndez, A. Thermogravimetric Analysis and Carbon Stability of Chars Produced from Slow Pyrolysis and Hydrothermal Carbonization of Manure Waste. *J. Anal. Appl. Pyrolysis* **2019**, *140*, 434–443. [[CrossRef](#)]
57. Channiwala, S.A.; Parikh, P.P. A Unified Correlation for Estimating HHV of Solid, Liquid and Gaseous Fuels. *Fuel* **2002**, *81*, 1051–1063. [[CrossRef](#)]
58. Qian, C.; Li, Q.; Zhang, Z.; Wang, X.; Hu, J.; Cao, W. Prediction of Higher Heating Values of Biochar from Proximate and Ultimate Analysis. *Fuel* **2020**, *265*, 116925. [[CrossRef](#)]
59. Smith, A.M.; Singh, S.; Ross, A.B. Fate of Inorganic Material during Hydrothermal Carbonisation of Biomass: Influence of Feedstock on Combustion Behaviour of Hydrochar. *Fuel* **2016**, *169*, 135–145. [[CrossRef](#)]
60. Mbugua Nyambura, S.; Li, C.; Li, H.; Xu, J.; Wang, J.; Zhu, X.; Feng, X.; Li, X.; Bertrand, G.V.; Ndiithi Ndumia, J.; et al. Microwave Co-Pyrolysis of Kitchen Food Waste and Rice Straw: Effects of Susceptor on Thermal, Surface, and Fuel Properties of Biochar. *Fuel* **2023**, *352*, 129093. [[CrossRef](#)]
61. Kongto, P.; Palamanit, A.; Ninduangdee, P.; Singh, Y.; Chanakaewsomboon, I.; Hayat, A.; Wae-hayee, M. Intensive Exploration of the Fuel Characteristics of Biomass and Biochar from Oil Palm Trunk and Oil Palm Fronds for Supporting Increasing Demand of Solid Biofuels in Thailand. *Energy Rep.* **2022**, *8*, 5640–5652. [[CrossRef](#)]
62. Igalavithana, A.D.; Mandal, S.; Niazi, N.K.; Vithanage, M.; Parikh, S.J.; Mukome, F.N.D.; Rizwan, M.; Oleszczuk, P.; Al-Wabel, M.; Bolan, N.; et al. Advances and Future Directions of Biochar Characterization Methods and Applications. *Crit. Rev. Environ. Sci. Technol.* **2017**, *47*, 2275–2330. [[CrossRef](#)]
63. Anand, A.; Gautam, S.; Ram, L.C. Feedstock and Pyrolysis Conditions Affect Suitability of Biochar for Various Sustainable Energy and Environmental Applications. *J. Anal. Appl. Pyrolysis* **2023**, *170*, 105881. [[CrossRef](#)]

64. Nelson, D.W.; Sommers, L.E. Total Carbon, Organic Carbon, and Organic Matter. In *Methods of Soil Analysis Part 3—Chemical Methods*; Soil Science Society of America and American Society of Agronomy: Madison, WI, USA, 1996; pp. 961–1009.
65. Wong, J.W.C.; Ogbonnaya, U.O. Biochar Porosity : A Nature-Based Dependent Parameter to Deliver Microorganisms to Soils for Land Restoration. *Environ. Sci. Pollut. Res.* **2021**, *28*, 46894–46909. [[CrossRef](#)] [[PubMed](#)]
66. Capareda, S.C. Comprehensive Biomass Characterization in Preparation for Conversion. In *Sustainable Biochar for Water and Wastewater Treatment*; Elsevier: Amsterdam, The Netherlands; Madison Wisconsin, WI, USA, 2022; pp. 1–37. ISBN 9780128222256.
67. Wang, C.; Wang, Y.; Herath, H.M.S.K. Polycyclic Aromatic Hydrocarbons (PAHs) in Biochar—Their Formation, Occurrence and Analysis: A Review. *Org. Geochem.* **2017**, *114*, 1–11. [[CrossRef](#)]
68. Greco, G.; Videgain, M.; Di Stasi, C.; Pires, E.; Manyà, J.J. Importance of Pyrolysis Temperature and Pressure in the Concentration of Polycyclic Aromatic Hydrocarbons in Wood Waste-Derived Biochars. *J. Anal. Appl. Pyrolysis* **2021**, *159*, 105337. [[CrossRef](#)]
69. Dumroese, R.K.; Page-Dumroese, D.S.; Pinto, J.R. Biochar Potential to Enhance Forest Resilience, Seedling Quality, and Nursery Efficiency. *Tree Plant. Notes* **2020**, *63*, 61–68.
70. Jarvis, J.M.; Page-Dumroese, D.S.; Anderson, N.M.; Corilo, Y.; Rodgers, R.P. Characterization of Fast Pyrolysis Products Generated from Several Western USA Woody Species. *Energy Fuels* **2014**, *28*, 6438–6446. [[CrossRef](#)]
71. Bakshi, S.; Banik, C.; Laird, D.A. Estimating the Organic Oxygen Content of Biochar. *Sci. Rep.* **2020**, *10*, 13082. [[CrossRef](#)]
72. Nogués, I.; Mazzurco Miritana, V.; Passatore, L.; Zacchini, M.; Peruzzi, E.; Carloni, S.; Pietrini, F.; Marabottini, R.; Chiti, T.; Massaccesi, L.; et al. Biochar Soil Amendment as Carbon Farming Practice in a Mediterranean Environment. *Geoderma Reg.* **2023**, *33*, e00634. [[CrossRef](#)]
73. Peuravuori, J.; Žbáňková, P.; Pihlaja, K. Aspects of Structural Features in Lignite and Lignite Humic Acids. *Fuel Process. Technol.* **2006**, *87*, 829–839. [[CrossRef](#)]
74. Cui, X.; Yan, H.; Zhao, P.; Yang, Y.; Xie, Y. Modeling of Molecular and Properties of Anthracite Base on Structural Accuracy Identification Methods. *J. Mol. Struct.* **2019**, *1183*, 313–323. [[CrossRef](#)]
75. Malysheva, V.Y.; Fedorova, N.I.; Nikitin, A.P. Spectral Analysis of Anthracite. *Coke Chem.* **2023**, *66*, 490–495. [[CrossRef](#)]
76. Liang, W.; Jiang, C.; Wang, G.; Ning, X.; Zhang, J.; Guo, X.; Xu, R.; Wang, P.; Ye, L.; Li, J.; et al. Research on the Co-Combustion Characteristics and Kinetics of Agricultural Waste Hydrochar and Anthracite. *Renew. Energy* **2022**, *194*, 1119–1130. [[CrossRef](#)]
77. Ouyang, Z.; Zhu, J.; Lu, Q. Experimental Study on Preheating and Combustion Characteristics of Pulverized Anthracite Coal. *Fuel* **2013**, *113*, 122–127. [[CrossRef](#)]
78. Zou, C.; Zhao, J.; Li, X.; Shi, R. Effects of Catalysts on Combustion Reactivity of Anthracite and Coal Char with Low Combustibility at Low/High Heating Rate. *J. Therm. Anal. Calorim.* **2016**, *126*, 1469–1480. [[CrossRef](#)]
79. Xiao, Y.; Meng, X.; Yin, L.; Li, Q.W.; Shu, C.M.; Tian, Y. Influence of Element Composition and Microcrystalline Structure on Thermal Properties of Bituminous Coal under Nitrogen Atmosphere. *Process Saf. Environ. Prot.* **2021**, *147*, 846–856. [[CrossRef](#)]
80. Hwang, T.; Neculita, C.M. In Situ Immobilization of Heavy Metals in Severely Weathered Tailings Amended with Food Waste-Based Compost and Zeolite. *Water. Air. Soil Pollut.* **2013**, *224*, 1388. [[CrossRef](#)]
81. Lu, X.; Pellechia, P.J.; Flora, J.R.V.; Berge, N.D. Influence of Reaction Time and Temperature on Product Formation and Characteristics Associated with the Hydrothermal Carbonization of Cellulose. *Bioresour. Technol.* **2013**, *138*, 180–190. [[CrossRef](#)]
82. Cueva Zepeda, L.; Griffin, G.; Shah, K.; Al-Waili, I.; Parthasarathy, R. Energy Potential, Flow Characteristics and Stability of Water and Alcohol-Based Rice-Straw Biochar Slurry Fuel. *Renew. Energy* **2023**, *207*, 60–72. [[CrossRef](#)]
83. Toloue Farrokh, N.; Suopajarvi, H.; Mattila, O.; Sulasalmi, P.; Fabritius, T. Characteristics of Wood-Based Biochars for Pulverized Coal Injection. *Fuel* **2020**, *265*, 117017. [[CrossRef](#)]
84. Ghidotti, M.; Fabbri, D.; Hornung, A. Profiles of Volatile Organic Compounds in Biochar: Insights into Process Conditions and Quality Assessment. *ACS Sustain. Chem. Eng.* **2017**, *5*, 510–517. [[CrossRef](#)]
85. Mandal, S.; Donner, E.; Vasileiadis, S.; Skinner, W.; Smith, E.; Lombi, E. The Effect of Biochar Feedstock, Pyrolysis Temperature, and Application Rate on the Reduction of Ammonia Volatilisation from Biochar-Amended Soil. *Sci. Total Environ.* **2018**, *627*, 942–950. [[CrossRef](#)] [[PubMed](#)]
86. Ronsse, F.; van Hecke, S.; Dickinson, D.; Prins, W. Production and Characterization of Slow Pyrolysis Biochar: Influence of Feedstock Type and Pyrolysis Conditions. *GCB Bioenergy* **2013**, *5*, 104–115. [[CrossRef](#)]
87. Al-Wabel, M.I.; Al-Omran, A.; El-Naggar, A.H.; Nadeem, M.; Usman, A.R.A. Pyrolysis Temperature Induced Changes in Characteristics and Chemical Composition of Biochar Produced from Conocarpus Wastes. *Bioresour. Technol.* **2013**, *131*, 374–379. [[CrossRef](#)]
88. Rehrah, D.; Reddy, M.R.; Novak, J.M.; Bansode, R.R.; Schimmel, K.A.; Yu, J.; Watts, D.W.; Ahmedna, M. Production and Characterization of Biochars from Agricultural By-Products for Use in Soil Quality Enhancement. *J. Anal. Appl. Pyrolysis* **2014**, *108*, 301–309. [[CrossRef](#)]
89. Vaughn, S.F.; Kenar, J.A.; Eller, F.J.; Moser, B.R.; Jackson, M.A.; Peterson, S.C. Physical and Chemical Characterization of Biochars Produced from Coppiced Wood of Thirteen Tree Species for Use in Horticultural Substrates. *Ind. Crops Prod.* **2015**, *66*, 44–51. [[CrossRef](#)]
90. Yargicoglu, E.N.; Sadasivam, B.Y.; Reddy, K.R.; Spokas, K. Physical and Chemical Characterization of Waste Wood Derived Biochars. *Waste Manag.* **2015**, *36*, 256–268. [[CrossRef](#)]
91. Fu, P.; Hu, S.; Xiang, J.; Sun, L.; Su, S.; Wang, J. Evaluation of the Porous Structure Development of Chars from Pyrolysis of Rice Straw: Effects of Pyrolysis Temperature and Heating Rate. *J. Anal. Appl. Pyrolysis* **2012**, *98*, 177–183. [[CrossRef](#)]

92. Buss, W.; Hilber, I.; Graham, M.C.; Mašek, O. Composition of PAHs in Biochar and Implications for Biochar Production. *ACS Sustain. Chem. Eng.* **2022**, *10*, 6755–6765. [[CrossRef](#)]
93. Schmidt, H.P.; Bucheli, T.D.; Kammann, C.; Glaser, B.; Abiven, S.; Leifeld, J. European Biochar Certificate—Guidelines for a Sustainable Production of Biochar. *Eur. Biochar Found.* **2016**, 1–22. [[CrossRef](#)]
94. Schleder, F.; Martín-Hernández, E.; Vaneeckhaute, C. Ensuring Safety Standards in Sewage Sludge-Derived Biochar: Impact of Pyrolysis Process Temperature and Carrier Gas on Micropollutant Removal. *J. Environ. Manag.* **2024**, *352*, 19964. [[CrossRef](#)] [[PubMed](#)]
95. De Luis, M.; Raventós, J.; González-Hidalgo, J.C. Factors Controlling Seedling Germination after Fire in Mediterranean Gorse Shrublands. Implications for Fire Prescription. *J. Environ. Manag.* **2005**, *76*, 159–166. [[CrossRef](#)] [[PubMed](#)]

Disclaimer/Publisher’s Note: The statements, opinions and data contained in all publications are solely those of the individual author(s) and contributor(s) and not of MDPI and/or the editor(s). MDPI and/or the editor(s) disclaim responsibility for any injury to people or property resulting from any ideas, methods, instructions or products referred to in the content.